ELSEVIER

Catalysis Today 72 (2002) 259–265

CATALYSIS TODAY

www.elsevier.com/locate/cattod

Involvement of catalyst materials in nonthermal plasma chemical processing of hazardous air pollutants

Shigeru Futamura*, Aihua Zhang, Hisahiro Einaga, Hajime Kabashima

Excited State Chemistry Group, Institute for Environmental Management Technology, National Institute of Advanced Industrial Science and Technology (AIST), AIST Tsukuba West, 16-1 Onogawa, Tsukuba, Ibaraki 305-8569, Japan

Abstract

Catalytic effects of metal oxides in nonthermal plasma chemical processing of hazardous air pollutants (HAPs) are discussed, relevant to their activities for the oxidation of HAPs in nonthermal plasma media and their selective control of active oxygen species derived from background O_2. In ferroelectric packed-bed reactors, the oxidation power of barium titanate ($BaTiO_3$) is not strong enough to oxidize HAPs and their carbon intermediates to CO_2. Only nitrous oxide (N_2O) was formed from background N_2 and lattice oxygen atoms in $BaTiO_3$. The catalytic effect of $BaTiO_3$ is negligible under aerated conditions. On the other hand, ozone (O_3) is formed from background O_2 in much higher concentrations in a silent discharge plasma reactor. Manganese dioxide (MnO_2)-catalyzed decomposition of O_3 promotes decomposition of benzene, which is less reactive than trichloroethylene and tetrachloroethylene. The acceleration of benzene consumption rate is ascribed to the promotion of its oxidative decomposition by the triplet oxygen atom. Catalytic control of in situ active oxygen species could be one of the most effective approaches to increase the energy efficiency of the nonthermal plasma reactor and to achieve the complete oxidation of the carbon atoms in HAPs.

Keywords: Hazardous air pollutants; Nonthermal plasma; Decomposition; Catalyst

1. Introduction

Nonthermal plasma chemical processing of hazardous air pollutants (HAPs) has been extensively investigated [1–15], and it has been clarified that this technique is extremely efficient in decomposing olefinic HAPs such as trichloroethylene ($Cl_2C{=}CHCl$, TCE) [5], tetrachloroethylene, and ethylene [6].

In use of ferroelectric pellet packed-bed reactors (FPR) [5–7] and a pulsed corona reactor [5], homolytic decomposition of excited HAPs is the major pathway in the absence or presence of oxidants such as O_2 and humidity in the background gas. In many cases, they deactivate excited electrons rather than promote oxidative decomposition of HAPs.

On the other hand, higher conversions have been obtained in the decomposition of volatile organic compounds (VOCs) in air with silent discharge plasma reactors (SDR) [13]. These findings suggest that the contributions of active oxygen species generated in nonthermal plasma are greatly affected by plasma-generating methods. Thus, combination of nonthermal plasma and catalysts (Fig. 1) can control the distribution of *in situ* active oxygen species such as ozone (O_3), oxygen atoms [$O(^1D)$ and $O(^3P)$], hydroxyl radical ($^{\bullet}OH$), and final oxidation products such as CO and CO_2. It has already been known that perovskite oxides such as barium titanate ($BaTiO_3$) packed in FPR (Fig. 1a) can act as catalysts in the partial oxidation of hydrocarbons at elevated temperatures [16], but

* Corresponding author. Tel.: +81-298-61-8497; fax: +81-298-61-8266.
E-mail address: s-futamura@aist.go.jp (S. Futamura).

0920-5861/02/$ – see front matter
PII: S0920-5861(01)00503-X

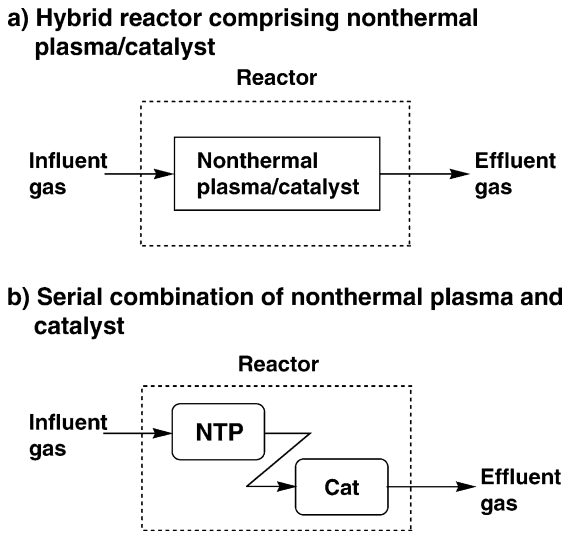

Fig. 1. Two modes of the nonthermal plasma/catalyst reactor: (a) hybrid reactor comprising nonthermal plasma/catalyst; (b) serial combination of nonthermal plasma and catyalyst.

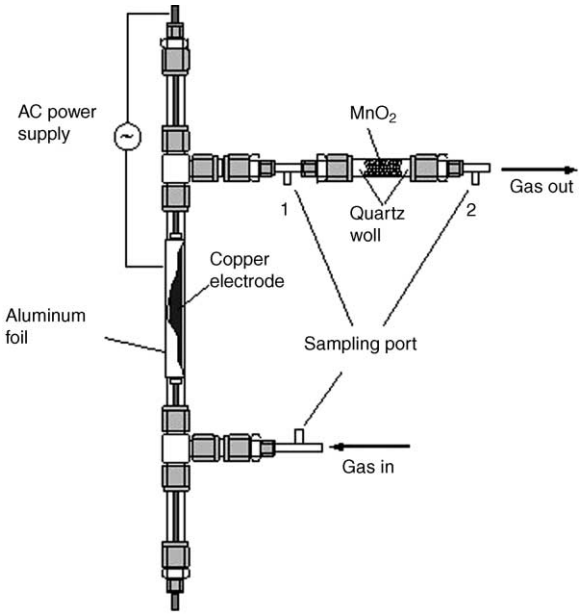

Fig. 2. Schematic of a silent discharge plasma (SDR)-MnO_2 reactor.

their catalytic effect in nonthermal plasma media has not been clarified yet. It has been reported that modification of the internal electrode of SDR with precious metals (Fig. 1a) is effective in activating CO_2, NO, and H_2O in nonthermal plasma [10].

Selective oxidation systems can be designed by serially combining a nonthermal plasma reactor and a catalyst layer (Fig. 1b). Catalytic control of active oxygen species in the second stage can promote the oxidative decomposition of VOCs.

This paper discusses the catalytic effect of $BaTiO_3$ used in FPR and metal oxide catalysts serially combined with SDR from the viewpoint of their involvement in the oxidation of N_2, CO, and VOCs.

2. Experimental

2.1. Characteristics of plasma reactors and experimental systems

Experiments were carried out in FPR and SDR reactors. FPR was a coaxial type. $BaTiO_3$ pellets ($\varepsilon = 5000$ at room temperature) of 1 mm in diameter were packed between the two concentric electrodes. The schematic and detailed specifications of FPR were described in our previous paper [8]. A SDR reactor used in this research was a tubular type consisting of a stainless steel rod coated with copper (o.d. 8.6 mmϕ) and an encircling glass tube (i.d. 10.6 mmϕ), which was wrapped with aluminum foil (100 mm wide) [13]. Fig. 2 shows the schematic of the SDR reactor equipped with a catalytic-bed at its exit. Both reactors were energized with 50 Hz ac up to 8–10 kV rms.

2.2. Plasma chemical decomposition of HAPs

The HAPs tested in this research were TCE, chloromethane (CH_3Cl), carbon tetrachloride (CCl_4), 1,1,1-trichloroethane ($Cl_3C–CH_3$), tetrachloroethylene ($Cl_2C{=}CCl_2$), bromomethane (CH_3Br), dibromomethane (CH_2Br_2), bromoethane ($CH_3–CH_2Br$), benzene, and CO. A HAP balanced with N_2 in a standard gas cylinder was introduced to the reactor through a Teflon tube by adjusting the flow rate and the concentrations of HAPs and O_2 with sets of mass flow controllers and a gas mixer.

Moisture was added to the gas by bubbling water with it, using a small volume water bath. The flowing gas lowered the water temperature by a few degrees

Celsius, but the estimated water vapor concentration remained nearly 2% by volume for all the experiments. Since the rest of the gas system remained at or above room temperature, there was no possibility of condensation.

The concentrations of CO and CO_2 were overestimated for the reactions under aerated conditions when they were carried out right after the runs under deareated condition. Their unexpectedly higher concentrations could be ascribed to the oxidative decomposition of carbonaceous materials deposited on the $BaTiO_3$ surface. Thus, after the runs under deaerated conditions, air was passed through FPR and SDR at 7 kV for 20 s to oxidatively remove the above carbon deposits.

2.3. Analysis

The values of primary power and applied voltage for FPR and SDR were measured with a digital powermeter (YOKOGAWA WT 110) and a digital wavemeter (SONY TEKTRONIX STA55W), respectively.

The volatile byproducts were identified by GC–MS [Shimadzu QP-5050A (EI, 70 eV)-GC-17A]. The VOC conversions and byproduct yields were determined by GC [GC 353 (GL Sciences)].

The concentrations of O_3 and NO_x were measured on a UV photometric analyzer, SOZ-6300 (Seki Electronics) and a luminescent NO_x analyzer, NOA 7000 (Shimadzu) [8], respectively.

3. Results and discussion

As a measure of the energy efficiency for FPR and SDR, specific energy density (SED) is used later (Eq. (1)), where primary power denotes the source power. The ratio of secondary power (power consumption in the reactor) to primary power is ca. 0.3 for both the reactors.

$$\text{SED (kJ/L)} = \frac{\text{primary power (kW)}}{\text{flow rate (l/s)}} \quad (1)$$

3.1. Catalytic effect of $BaTiO_3$ in FPR

Perovskite oxides such as $BaTiO_3$ are known to catalyze the partial oxidation of hydrocarbons at temperatures higher than 600 K [16]. The behavior of $BaTiO_3$ in nonthermal plasma is interesting because electron temperature there reaches as high as 40,000 K [17] with gas temperature around at ambient temperature. Figs. 3 and 4 show the background effect on the conversions of TCE and benzene. For each of them, almost the same conversions are obtained in dry air and in dry nitrogen. Since the anaerobic cleavage of their covalent bonds can occur very fast, contributions of

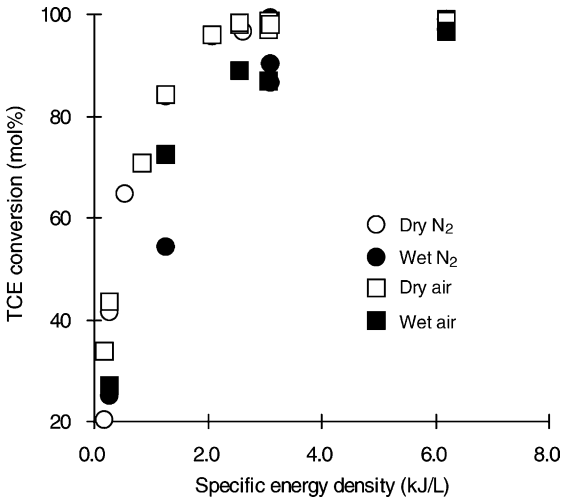

Fig. 3. Background gas effect on TCE conversion: reactor, FPR; TCE concentration, 1000 ppm.

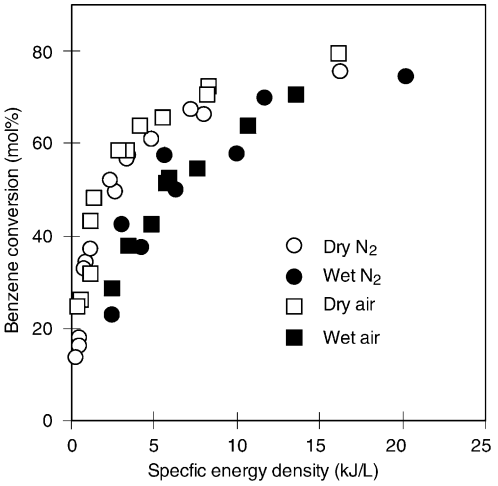

Fig. 4. Background effect on benzene conversion: reactor, FPR; benzene concentration, 500 ppm.

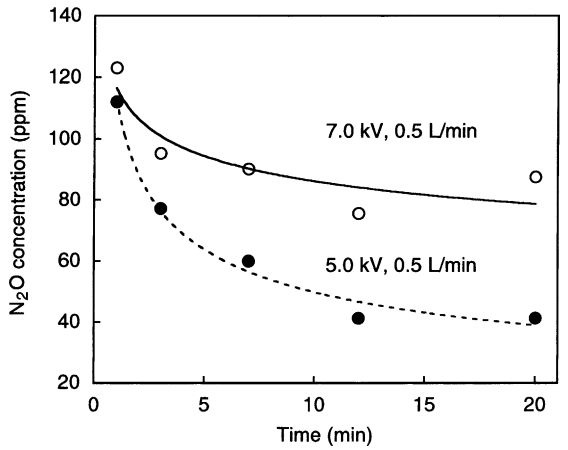

Fig. 5. Time profile of N_2O formation in dry N_2: reactor, FPR.

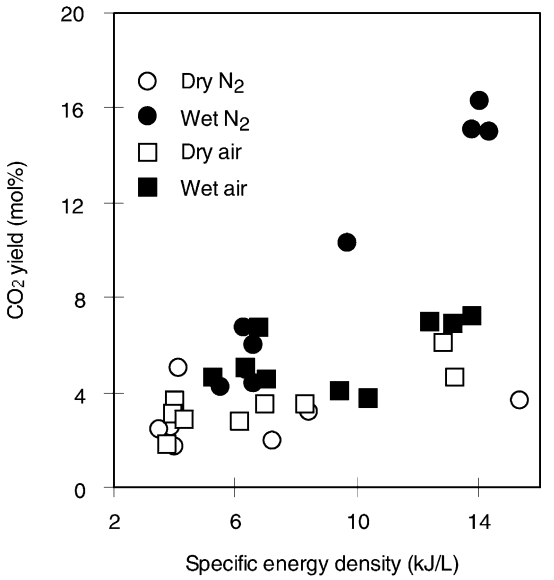

Fig. 6. Background effect on the CO oxidation: reactor, FPR; CO concentration, 1000 ppm.

catalytic oxidative decomposition by some active oxygen species and $BaTiO_3$ are negligible. Humidity depressed the decomposition of TCE and benzene. It is less likely that $BaTiO_3$ catalyzes the formation of $^{\bullet}OH$ from water and $O(^1D)$.

Nitrogen oxides are formed as byproducts in VOC decomposition, and the suppression of their formation is one of the greatest issues at this stage. With FPR in nitrogen, NO_x formation could be neglected, but considerable amounts of N_2O were generated. Fig. 5 shows that N_2O concentration decreases with reaction time and levels off at different concentrations in N_2, depending on the magnitude of applied voltage. These findings suggest that oxygen atoms on the surface of $BaTiO_3$ are initially consumed in N_2O formation, and at stationary states, even lattice oxygen atoms in $BaTiO_3$ are consumed in the reaction. N_2O formation could not be observed when FPR was not energized. Thus, it seems that nonthermal plasma excites oxygen atoms in $BaTiO_3$. This type of active oxygen species can be also used in the oxidation of carbon fragments derived from the decomposition of various VOCs. However, CO formation predominates under these conditions with poor carbon balances. In the presence of gaseous oxygen, the amounts of NO, NO_2, and N_2O increase with O_2 content and SED. Therefore, contributions of surface reactions are small in the presence of gaseous oxygen even with FPR.

CO is one of the least reactive HAPs in nonthermal plasma. Fig. 6 shows that CO_2 yields are very poor in dry nitrogen and in dry air. The CO_2 yields increments did not exceed 15 mol% even in the presence of humidity. In the oxidation of CO to CO_2, $BaTiO_3$ cannot act as an effective catalyst. Even in the presence of O_2, the molar ratios of CO to CO_x decreased with the increase of HAP conversion in dry air (Table 1). It has been reported that CO_2 yields cannot be enhanced by using $BaTiO_3$ coated with precious metals [4] or physical mixtures of $BaTiO_3$ and M/Al_2O_3 [9].

3.2. Synergism of nonthermal plasma and MnO_2 catalyst

With FPR, O_3 formation was negligible even in air without VOCs, and its maximum concentration was lower than 1.5 ppm at 8 kJ/l of SED. On the other hand, considerable amounts of O_3 were formed with SDR at higher flow rates (Fig. 7). At 0.5 L/min, however, O_3 concentration tended to saturate, suggesting that an equilibrium is established for the formation and decomposition of O_3. Under normal operating conditions of SDR, flow rate was lower than 0.5 L/min, and O_3 concentration was not high enough to decompose 1000 ppm of VOCs at residence times shorter than 1.8 s [13].

Table 1
Relationship between HAP conversion and CO_2 selectivity in dry air[a]

HAP	Lowest HAP conversion (mol%)	$[CO_2]/\{[CO] + [CO_2]\}$	Highest HAP conversion (mol%)	$[CO_2]/\{[CO] + [CO_2]\}$
PhH	32	0.51	79	0.46
$CH_2{=}CH_2$	30	0.46	98	0.38
CH_3Cl	21	0.33	76	0.28
CCl_4	32	0.22	59	0.13
$Cl_3C–CH_3$	21	0.46	96	0.32
$Cl_2C{=}CHCl$	43	0.39	99	0.30
$Cl_2C{=}CCl_2$	29	0.45	98	0.30
CH_3Br	16	0.37	73	0.32
CH_2Br_2	17	0.27	95	0.25
CH_3CH_2Br	21	0.45	61	0.37

[a] Reactor: FPR.

From the viewpoint of air pollution control, synergism of nonthermal plasma and catalysts should be achieved in the selective generation of active oxygen species and complete oxidation of VOC carbons to CO_2 because of the large magnitude of reaction energy available in nonthermal plasma itself. The catalytic activity of $BaTiO_3$ could not be enhanced in nonthermal plasma with FPR, which urged us to explore the synergistic effect of silent discharge plasma and catalysts. According to our previous data, no correlation was observed between the amount of O_3 formed from gaseous oxygen and the conversions of VOCs such as TCE and CH_3Br under aerated conditions.

However, we have newly found that benzene conversion was greatly increased by serially connecting the MnO_2 pellet (mesh 22–42) layer (i.d. 10 mmϕ × 105 mm) to the outlet of SDR (Fig. 8). When 106 ppm of benzene in dry air was decomposed at 0.25 L/min of gas flow rate and at 0.6 kJ/L of SED with SDR, benzene conversion is 16% along with 398 ppm of O_3 as a byproduct. When the same reactant gas is passed through the SDR-MnO_2 hybrid reactor under the same conditions, benzene conversion was increases to 64% with no O_3 present. Fig. 9 shows that ca. 10% of benzene was decomposed at the exit of SDR with 400 ppm of O_3 formed from O_2 when

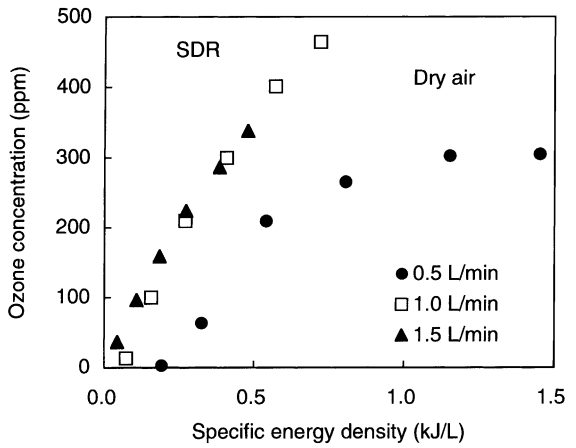

Fig. 7. Effect of gas flow rate on the O_3 formation behavior from air with SDR.

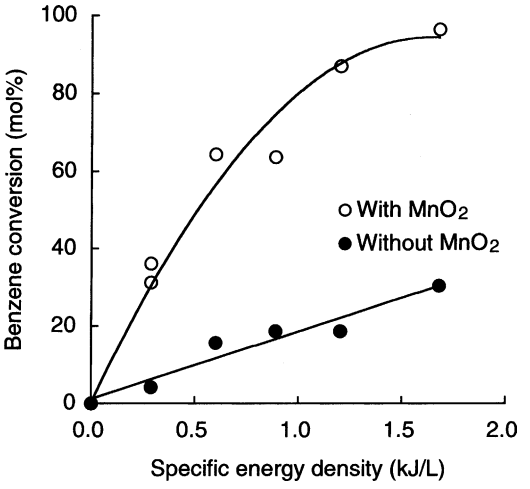

Fig. 8. Catalytic effect of MnO_2 in the decomposition of benzene in air: benzene concentration, 106 ppm; MnO_2, 2 g.

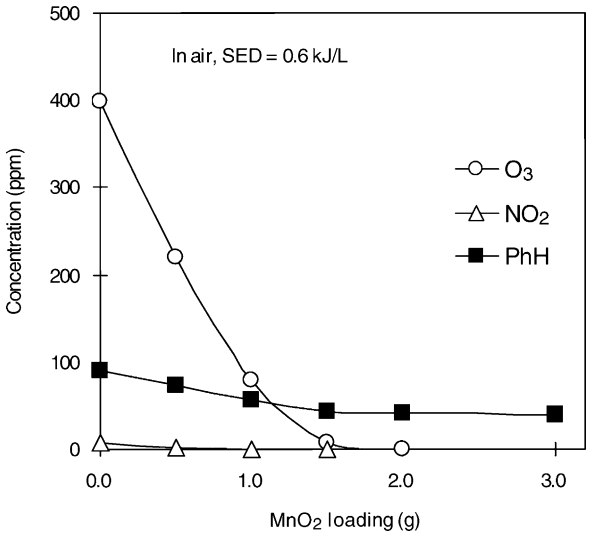

Fig. 9. Effect of MnO_2 amount on the decomposition of benzene and O_3 in air: benzene concentration 106 ppm.

no MnO_2 is used. Compared to the concentrations of benzene and O_3, that of NO_2 was negligible. The decomposition of ozone and benzene is simultaneously promoted with an increase of MnO_2 loading. About 10 molar equivalents of O_3 was consumed in the decomposition of benzene. This value was smaller than the stoichiometric one needed for the complete oxidation of benzene by O_3. This fact is ascribed to formation of CO from benzene and the involvement of O_2 in the further oxidation of reaction intermediates. These findings clearly show that MnO_2 promoted O_3 decomposition, accelerating the oxidative decomposition of benzene.

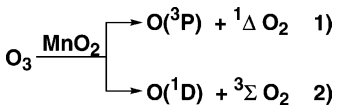

Fig. 10. Plausible mechanism for MnO_2-catalyzed decomposition of O_3.

In the TCE decomposition with SDR, its conversion was higher in dry air than in dry N_2 without MnO_2 [13]. $O(^3P)$ is much more reactive with TCE [$k = 5.3 \times 10^{-13}$ (cm^3 per molecule per second)] [18] than O_3 is [$k = 5.0 \times 10^{-20}$ (cm^3 per molecule per second)] [19]. According to Eliasson et al. [20], $O(^3P)$ is produced in higher concentrations than $O(^1D)$ in the initial stage of a microdischarge generated with a type of SDR. It is also well known that $O(^3P)$ acts as a monooxygenating agent toward aromatic hydrocarbons [21]. Although the branching ratio for Eqs. (1) and (2) in Fig. 10 is unknown in the reaction system of benzene decomposition, the responsible species could be $O(^3P)$ rather than $O(^1D)$. It is least likely that NO_2 was involved in the oxidative decomposition of benzene.

On the other hand, O_3 decomposition was not observed when the O_3 (808 ppm)-containing air was passed through the $BaTiO_3$ pellet layer instead of MnO_2 at ambient temperature. These findings show that $BaTiO_3$ is inactive in O_3 decomposition at ambient temperature. Compared to the findings with SDR, much lower concentrations of O_3 with FPR cannot be rationalized by its fast noncatalytic decomposition in FPR. One possibility is that O_3 reacts with $BaTiO_3$-surface oxygen atoms activated in nonthermal plasma.

Table 2
Effect of SED and humidity on benzene conversion and selectivities of CO and CO_2[a]

Run	SED (kJ/L)	Relative humidity (%)	Benzene conversion (mol%)	Selectivity (mol%)[b]		CO_x yield (mol%)
				CO_2	CO	
1	0.3	0	36.2	73	27	44
2	0.6	0	64.4	72	28	51
3	1.5	0	99.5	71	29	65
4	4.2	0	99.8	70	30	80
5	1.5	50	33.4	91	9	71
6	4.2	50	93.1	90	10	81

[a] Reactor: SDR.
[b] $[CO_x$ ($x = 1$ or 2)]/{[CO] + {CO_2]}.

O_3 formation behavior highly depends on nonthermal plasma-generating methods, and the use of pertinent catalysts is necessary to utilize O_3 as an oxidant precursor in VOC decomposition.

Table 2 shows the effects of SED and humidity on the benzene conversions and the selectivities of CO and CO_2 defined as $[CO_x\ (x = 1 \text{ or } 2)]/\{[CO] + [CO_2]\}$. Compared to FPR, higher CO_2 selectivities are obtained with SDR (Runs 1–4). Both of benzene conversion and CO_2 selectivity were greatly enhanced by air humidification (Run 6). If the ratio of secondary power to primary power can be increased, benzene could be oxidized to CO_2 with much less energy under humid conditions.

4. Conclusions

Catalytic effects of metal oxides have been discussed with two different types of nonthermal plasma reactors: ferroelectric packed-bed (FPR) and silent discharge (SDR). Barium titanate in FPR can act as a monooxygenating agent under deaerated conditions, but its catalytic activity is low in the processes such as oxidation of VOC carbons and CO. N_2O is produced from lattice oxygen atoms in barium titanate and background N_2, but the contribution of this reaction is negligible under aerated conditions. Compared to FPR, abundant O_3 is generated from air with SDR, and it is possible to utilize it as an oxidant precursor in the oxidative decomposition of benzene by combining SDR with a layer of catalyst such as MnO_2. Benzene is effectively oxidized to CO_2 in humid air in a SDR-MnO_2 reactor.

Acknowledgements

This research was financially supported by the Grants-in-Aid “Global Environmental Research on the Development of the Technologies for Decomposition of Brominated Organic Compounds” and “Environmental Research for Pollution Control and Nature Conservation on the Reduction of Benzene Emission” of Environment Agency, Japan.

References

[1] T. Yamamoto, P.A. Lawless, M.K. Owen, D.S. Ensor, C. Boss, in: B.M. Penetrante, S.E. Schultheis (Eds.), Non-Thermal Plasma Techniques for Pollution Control, Vol. 34, Part B, NATO ASI Series, Springer, Berlin, 1993, p. 139.
[2] D. Evans, L.A. Rosocha, G.K. Anderson, J.J. Coogan, M.J. Kushner, J. Appl. Phys. 74 (1993) 5378.
[3] T. Yamamoto, J.S. Chang, A.A. Berezin, H. Kohno, S. Honda, J. Adv. Oxid. Technol. 1 (1996) 67.
[4] T. Yamamoto, K. Mizuno, I. Tamori, A. Ogata, M. Nifuku, M. Michalska, G. Prieto, IEEE Trans. Ind. Applicat. 32 (1996) 100.
[5] S. Futamura, T. Yamamoto, IEEE Trans. Ind. Applicat. 33 (1997) 447.
[6] S. Futamura, A. Zhang, T. Yamamoto, J. Electrostat. 42 (1997) 51.
[7] S. Futamura, A. Zhang, G. Prieto, T. Yamamoto, IEEE Trans. Ind. Applicat. 34 (1998) 967.
[8] S. Futamura, A. Zhang, T. Yamamoto, in: Proceedings of the Conference Record of 33rd IEEE-IAS Annual Meeting, St. Louis, MO, 12–15 October 1998, p. 1794.
[9] A. Ogata, K. Yamauchi, K. Mizuno, S. Kushiyama, T. Yamamoto, Conf. Record of 33rd IEEE-IAS Annual Meeting, St. Louis, MO, 12–15 October 1998, p. 1801.
[10] S.L. Suib, S.L. Brock, M. Marquez, J. Luo, H. Matsumoto, Y. Hayashi, J. Phys. Chem. B 102 (1998) 9661.
[11] S. Futamura, A. Zhang, T. Yamamoto, IEEE Trans. Ind. Applicat. 35 (1999) 760.
[12] A. Zhang, S. Futamura, T. Yamamoto, J. Air Waste Manage. Assoc. 49 (1999) 174.
[13] S. Futamura, H. Einaga, A. Zhang, in: Proceedings of the Conference Record of 34th IEEE-IAS Annual Meeting, 3–7 October 1999, Phoenix, AZ, p. 1105.
[14] S. Futamura, A. Zhang, H. Einaga, Preprints, Am. Chem. Soc. Div. Petroleum Chem. 45 (2000) 411.
[15] H. Einaga, T. Ibusuki, S. Futamura, in: Proceedings of the Conference Record of 35th IEEE-IAS Annual Meeting, 8–12 October 2000, Rome, p. 858.
[16] T. Shimizu, Catal. Rev.-Sci. Eng. 34 (1992) 355.
[17] J.S. Chang, in: J.S. Chang, A.J. Kelly, J.M. Crowley, (Eds.), Handbook of Electrostatic Processes, Dekker, New York, 1995, p. 157.
[18] W.-D. Chang, S.M. Senkan, Env. Sci. Technol. 23 (1989) 442.
[19] D.R. Lide (Ed.), CRC Handbook of Chemistry and Physics, 77th Edition, CRC Press, Boca Raton, 1996, pp. 5–117.
[20] B. Eliasson, U. Kogelschatz, J. Chim. Phys. 83 (1986) 279.
[21] R.J. Cvetanovic, Adv. Photochem. 1 (1963) 115.